$\Lambda_b \to \Lambda(\to p\pi^-)\ell^+\ell^-$ as probe of *CP*-violating new physics

Diganta Das,[1] Jaydeb Das,[2] Girish Kumar,[3] and Niladribihari Sahoo[4]

[1]*Center for Computational Natural Sciences and Bioinformatics, International Institute of Information Technology, Hyderabad 500 032, India*

[2]*Department of Physics and Astrophysics, University of Delhi, Delhi 110007, India*

[3]*Department of Physics, National Taiwan University, Taipei 10617, Taiwan*

[4]*School of Physics and Astronomy, University of Birmingham, Birmingham B15 2TT, United Kingdom*

(Received 25 November 2022; accepted 9 June 2023; published 5 July 2023)

We investigate the possible sizes of all the *CP*-violating asymmetries offered by the angular distribution of rare decay $\Lambda_b \to \Lambda(\to p\pi^-)\ell^+\ell^-$ in the Standard Model and new physics scenarios motivated by the recent $b \to s\ell^+\ell^-$ anomalies. We work in a model-independent effective theory framework and discuss the sensitivity of *CP* asymmetries to new $O_{9,10}$ operators and their chirality flipped counterparts. We find that the size of many of the *CP* asymmetries can be at the level of a few percent in new physics scenarios consistent with current $b \to s\ell^+\ell^-$ data at a level of 1σ. We emphasize that measurements of these *CP* asymmetries can be used to discriminate different new physics scenarios in $b \to s\ell^+\ell^-$.

DOI: 10.1103/PhysRevD.108.015001

I. INTRODUCTION

A major motivation for going beyond the Standard Model (SM) is to find new sources of charge-parity violation (*CPV*) required for the explanation of baryonic asymmetry of the Universe (BAU). The SM possesses two *CPV* sources: the Cabibbo-Kobayashi-Maskawa (CKM) phase (related to weak interactions), and a strong *CP* phase that is severely constrained by the upper limit of the neutron electric dipole moment measurement [1]. So far, all experimental observations of *CPV* have been in the quark sector and are consistent with the CKM mechanism. However, it is well known that the SM fails to satisfy the Sakharov's conditions [2] needed for explaining the BAU. Therefore, investigations of experimentally accessible *CP*-violating observables offering excellent sensitivity to physics beyond the SM are highly motivated.

At the luminosity frontier of new physics (NP) searches, the physical processes with underlying quark current $b \to s\ell^+\ell^-$ transitions have been of particular interest in recent times. The measurements of several observables related to processes $B \to K^{(*)}\mu^+\mu^-$ [3–6], $B_s \to \phi\mu^+\mu^-$ [7,8], show deviations from the SM expectation. On the other hand, the recently reported measurements of lepton flavor universality (LFU) ratios $R_{K^{(*)}} = \mathcal{B}(B \to K^{(*)}\mu^+\mu^-)/\mathcal{B}(B \to K^{(*)}e^+e^-)$ [9,10] by the LHCb [11,12], which are updates of previous measurements [13–16], agree with the SM. However, the latest global likelihood analyses of $b \to s\ell^+\ell^-$ that include the latest $R_{K^{(*)}}$ measurements still show large preference for the NP hypothesis over the SM [17–19][1] (also see Ref. [36]. which discusses the impact of long-distance contributions associated with charm loops). Although these results indicate the presence of a lepton flavor universal NP, it is also worth mentioning that there may still be sufficient room for LFU violation if the NP is associated with *CP* violation [37]. These anomalies, collectively known as neutral-current *B* anomalies, will be tested rigorously in the upcoming measurements with more data and, if confirmed, would be indisputable evidence of NP in $b \to s\ell^+\ell^-$ transitions.

The aforementioned anomalies, if confirmed, say nothing about the *CP* nature of the underlying NP as the concerned $b \to s\ell^+\ell^-$ observables are *CP* averaged. However, $b \to s\ell^+\ell^-$ decays also offer a multitude of observables which are highly sensitive to the *CP* nature of NP, aided by the fact that in the SM the $b \to s\ell^+\ell^-$ transitions are doubly Cabibbo suppressed [38]. Combined measurements of *CP*-violating and *CP*-conserving observables therefore provide a more powerful

[1]Earlier fits can be found, for example, in Refs. [20–35].

method to understand the CP properties of NP. In the literature, several works have investigated the CP asymmetries in $B \to K^* \mu^+ \mu^-$ angular distributions to probe NP [17,38–45] and, as illustrated in Ref. [43], the CP asymmetries are capable of distinguishing between NP models that address the $b \to s\ell^+\ell^-$ anomalies.

If the observed deviation in the $b \to s\ell^+\ell^-$ is indeed due to unambiguous short-distance NP then it would, in principle, also affect all semileptonic processes with the same underlying current. One important example is the baryonic decay $\Lambda_b \to \Lambda(\to p\pi^-)\ell^+\ell^-$ for an unpolarized Λ_b, which is the topic of this paper. There are several benefits of studying this decay. The angular distribution of $\Lambda_b \to \Lambda(\to p\pi^-)\ell^+\ell^-$, similar to its mesonic counterpart $B \to K^*(\to K\pi)\ell^+\ell^-$, offers a large number of CP-conserving as well as CP-violating angular asymmetries that provide complementary information about NP in $b \to s\ell^+\ell^-$ [46]. The secondary decay $K^* \to K\pi$ in mesonic mode $B \to K^*(\to K\pi)\ell^+\ell^-$ is a strong decay and therefore it conserves parity. On the other hand, the decay $\Lambda \to p\pi^-$ in the baryonic mode is a parity violating weak decay; this characteristic will play a key role in constructing several CP-violating asymmetries in $\Lambda_b \to \Lambda(\to p\pi^-)\ell^+\ell^-$, as discussed later in this paper. Furthermore, as pointed out in Ref. [47], $\Lambda_b \to \Lambda$ form factors, in comparison to $B \to K^*$, are more suitable to be computed with higher precision using lattice QCD due to the stability of Λ under strong interactions.

The first observation of $\Lambda_b \to \Lambda(\to p\pi^-)\ell^+\ell^-$ was reported by the CDF [48]. The recent angular analysis of unpolarized[2] $\Lambda_b \to \Lambda(\to p\pi^-)\ell^+\ell^-$ by the LHCb indicates a branching ratio that is smaller than the SM expectation [52], a pattern also observed in the $B \to K^{(*)}\mu^+\mu^-$, $B_s \to \phi\mu^+\mu^-$ modes. There are extensive theoretical works on the model-independent study of $\Lambda_b \to \Lambda(\to p\pi^-)\ell^+\ell^-$ in the SM and beyond [46,47,50,53–75]. These works mostly focus on CP-conserving angular observables. To the best of our knowledge, angular observables which discriminate the decay with its CP-conjugated mode $\bar{\Lambda}_b \to \bar{\Lambda}(\to \bar{p}\pi^+)\ell^+\ell^-$ and their role in the probe of NP in $b \to s\ell^+\ell^-$ have not been discussed yet. This paper investigates the prospects of CP asymmetries associated with the baryonic mode and assesses their sensitivity to CP-violating NP. We give descriptions of all possible CP-violating asymmetries that are at disposal from $\Lambda_b \to \Lambda(\to p\pi^-)\ell^+\ell^-$ angular distribution. Focusing on the muonic mode, we identify the sensitivity of these asymmetries to various NP Wilson coefficients (WCs) and show that the measurement of CP asymmetries in $\Lambda_b \to \Lambda(\to p\pi^-)\mu^+\mu^-$ can be used to distinguish various NP solutions that are favored by current global $b \to s\mu^+\mu^-$ data.

The paper is organized as follows. We begin the next section with a description of the model-independent effective framework relevant for the study of $b \to s\ell^+\ell^-$ transitions. In Sec. III we define the full angular distribution of both $\Lambda_b \to \Lambda(\to p\pi^-)\mu^+\mu^-$ and its CP-conjugated mode, and discuss the subtleties the CP properties of the secondary decay of $\Lambda(\bar{\Lambda})$ particles bring in, defining the corresponding angular coefficients. In Sec. IV we define all the CP-violating asymmetries of the Λ_b decay angular distribution and present our main numerical results. Finally, we offer our conclusions in Sec. V.

II. $b \to s\ell^+\ell^-$ EFFECTIVE LAGRANGIAN

In the SM, the $b \to s\ell^+\ell^-$ decays arise at the loop level only. The Lagrangian relevant at the scale $\mu = m_b$ is given by [41]

$$\mathcal{L}_{\rm eff} = \frac{4G_F}{\sqrt{2}}\lambda_t \Big[C_1 O_1^c + C_2 O_2^c + \sum_{i=3}^{6} C_i O_i + \sum_{i=7}^{10} (C_i O_i + C_i' O_i') + (\lambda_u/\lambda_t)\{C_1(O_1^c - O_1^u) + C_2(O_2^c - O_2^u)\}\Big], \quad (1)$$

where G_F is the Fermi's constant, and $\lambda_i = V_{ib}V_{is}^*$, where V_{ij} denotes the CKM matrix element. The WCs C_i contain information about short-distance physics associated with local operators O_i. For the discussion of the $b \to s\ell^+\ell^-$ transition, $O_{7,9,10}$ are the dominant operators which we list below. Denoting the chiral projectors as $P_{L,R} = (1 \mp \gamma_5)/2$, one has

$$O_7 = \frac{e}{16\pi^2} m_b [\bar{s}\sigma_{\mu\nu} P_R b] F^{\mu\nu}, \quad (2)$$

$$O_9 = \frac{e^2}{16\pi^2} [\bar{s}\gamma_\mu P_L b][\bar{\ell}\gamma^\mu \ell],$$
$$O_{10} = \frac{e^2}{16\pi^2} [\bar{s}\gamma_\mu P_L b][\bar{\ell}\gamma^\mu \gamma_5 \ell], \quad (3)$$

with $C_7(m_b) \simeq -0.3$ and $C_9(m_b) \approx -C_{10}(m_b) \simeq 4.2$ in the SM. Note that the primed operators are the chirality flipped counterparts of the SM operators, and in the SM their contributions (C_i') are vanishing. The operators $O_{1\text{–}6}$ are four-quark operators related to decays $b \to s\bar{q}q$, and O_8 is dipole operator related to radiative decay $b \to s\gamma$. Their explicit form can be found, for example, in Refs. [76–78]. These operators contribute to the $b \to s\ell^+\ell^-$ through quark loops. It is customary to include

[2]A full angular analysis of $\Lambda_b \to \Lambda(\to p\pi^-)\ell^+\ell^-$ with polarized Λ_b has been performed by LHCb in Ref. [49]. Predictions in the SM and beyond for polarized Λ_b decay $\Lambda_b \to \Lambda(\to p\pi^-)\ell^+\ell^-$ can be found in Refs. [50,51].

TABLE I. Values of $b \to s\ell^+\ell^-$ WCs in the SM at $\mu = 4.2$ GeV taken from Ref. [47].

C_1	C_2	C_3	C_4	C_5	C_6	C_7	C_8	C_9	C_{10}
−0.2877	1.0101	−0.0060	−0.0860	0.0004	0.0011	−0.3361	−0.1821	4.2745	−4.1602

their contribution in the effective WCs $C_{7(9)}^{\rm eff}$ of operators $O_{7(9)}$. These effective coefficients at next-to-next-to-leading logarithmic are given as

$$C_7^{\rm eff} = C_7 - \frac{1}{3}\left(C_3 + \frac{4}{3}C_4 + 20C_5 + \frac{80}{3}C_6\right) - \frac{\alpha_s}{4\pi}((C_1 - 6C_2)F_{1,c}^7(q^2) + C_8F_8^7(q^2)), \tag{4}$$

$$\begin{aligned} C_9^{\rm eff} = {} & C_9 + \frac{4}{3}C_3 + \frac{64}{9}C_5 + \frac{64}{27}C_6 \\ & + h(q^2,0)\left(-\frac{1}{2}C_3 - \frac{2}{3}C_4 - 8C_5 - \frac{32}{3}C_6\right) \\ & + h(q^2,m_b)\left(-\frac{7}{2}C_3 - \frac{2}{3}C_4 - 38C_5 - \frac{32}{3}C_6\right) \\ & + h(q^2,m_c)\left(\frac{4}{3}C_1 + C_2 + 6C_3 + 60C_5\right) \\ & - \frac{\alpha_s}{4\pi}(C_1F_{1,c}^9(q^2) + C_2F_{2,c}^9(q^2) + C_8F_8^9(q^2)) \\ & + \frac{\lambda_u}{\lambda_t}\left(\frac{4}{3}C_1 + C_2\right)(h(q^2,m_c) - h(q^2,0)). \end{aligned} \tag{5}$$

The functions $h(a,b)$ and $F_8^{7,9}(q^2)$ are given in Ref. [79], and the functions $F_{i,c}^{7,9}(q^2)$ $(i = 1,\ 2)$ are provided in Refs. [80,81]. Note that the quark masses appearing in Eqs. (4) and (5) are in the pole scheme, and the corresponding values ($m_b^{\rm pole} = 4.74174$ GeV, $m_c^{\rm pole} = 1.5953$ GeV) are taken from Ref. [47]. The numerical values of SM Wilson coefficients contributing to $b \to s\ell^+\ell^-$ are given in Table I.

There are $(\bar{s}b)(\bar{\ell}\ell)$ operators with scalar and tensor structures which may arise in NP; but scalar operators are highly constrained from $B_s \to \mu^+\mu^-$ data [82,83]. Furthermore, since the current global fits to $b \to s\mu^+\mu^-$ data strongly prefer NP in WCs of left-handed (axial)vector operators in Eq. (3), we will also neglect NP tensor operators for the simplicity of the analysis.

III. ANGULAR DISTRIBUTION

Assuming the Λ_b to be unpolarized, the fourfold differential angular distributions for $\Lambda_b \to \Lambda(\to p\pi^-)\ell^+\ell^-$ are given by [46]

$$\begin{aligned} & \frac{{\rm d}^4\Gamma}{{\rm d}q^2 {\rm d}\cos\theta_\ell {\rm d}\cos\theta_\Lambda {\rm d}\phi} \\ & = \frac{3}{8\pi}[(K_{1ss}\sin^2\theta_\ell + K_{1cc}\cos^2\theta_\ell + K_{1c}\cos\theta_\ell) \\ & \quad + (K_{2ss}\sin^2\theta_\ell + K_{2cc}\cos^2\theta_\ell + K_{2c}\cos\theta_\ell)\cos\theta_\Lambda \\ & \quad + (K_{3sc}\sin\theta_\ell\cos\theta_\ell + K_{3s}\sin\theta_\ell)\sin\theta_\Lambda\sin\phi \\ & \quad + (K_{4sc}\sin\theta_\ell\cos\theta_\ell + K_{4s}\sin\theta_\ell)\sin\theta_\Lambda\cos\phi]. \end{aligned} \tag{6}$$

The distribution is completely described by four variables: the invariant lepton mass squared (q^2) and three Euler angles, θ_ℓ, θ_Λ, and ϕ. In the rest frame of Λ_b, the daughter baryon is assumed to travel along the $+z$ axis. The θ_Λ is the angle made by the proton with the $+z$ axis in the rest frame of the Λ, θ_ℓ is the angle made by the ℓ^- with respect to the $+z$ axis in the rest frame of the lepton pair, and ϕ defines the angle in the rest frame of Λ_b between planes containing $p\pi^-$ and the lepton pair. Denoting the mass of Λ_b, Λ, and charged lepton ℓ as m_{Λ_b}, m_Λ, and m_ℓ, respectively, the physical region of the decay process is defined by the following values:

$$q^2 \in [4m_\ell^2, (m_{\Lambda_b} - m_\Lambda)^2], \qquad \cos\theta_\Lambda \in [-1,1], \qquad \cos\theta_\ell \in [-1,1], \qquad \phi \in [0, 2\pi]. \tag{7}$$

In Eq. (6), the angular coefficients K_i are functions of q^2. These are conveniently described in terms of $\Lambda_b \to \Lambda$ transversity amplitudes, $A_i^{L,R}(q^2)$ as follows:

$$K_{1ss} = \frac{1}{4}(2|A_{\parallel_0}^R|^2 + |A_{\parallel_1}^R|^2 + 2|A_{\perp_0}^R|^2 + |A_{\perp_1}^R|^2 + \{R \leftrightarrow L\}), \tag{8}$$

$$K_{1cc} = \frac{1}{2}(|A_{\parallel_1}^R|^2 + |A_{\perp_1}^R|^2 + \{R \leftrightarrow L\}), \tag{9}$$

$$K_{1c} = -{\rm Re}(A_{\perp_1}^R A_{\parallel_1}^{*R} - \{R \leftrightarrow L\}), \tag{10}$$

$$K_{2ss} = \frac{\alpha_\Lambda}{2}{\rm Re}(2A_{\perp_0}^R A_{\parallel_0}^{*R} + A_{\perp_1}^R A_{\parallel_1}^{*R} + \{R \leftrightarrow L\}), \tag{11}$$

$$K_{2cc} = \alpha_\Lambda {\rm Re}(A_{\perp_1}^R A_{\parallel_1}^{*R} + A_{\perp_1}^L A_{\parallel_1}^{*L}), \tag{12}$$

$$K_{2c} = -\frac{\alpha_\Lambda}{2}{\rm Re}(|A_{\perp_1}^R|^2 + |A_{\parallel_1}^R|^2 - \{R \leftrightarrow L\}), \tag{13}$$

$$K_{3sc} = \frac{\alpha_\Lambda}{\sqrt{2}}{\rm Im}(A_{\perp_1}^R A_{\perp_0}^{*R} - A_{\parallel_1}^R A_{\parallel_0}^{*R} + \{R \leftrightarrow L\}), \tag{14}$$

$$K_{3s} = \frac{\alpha_\Lambda}{\sqrt{2}}\mathrm{Im}(A^R_{\perp_1}A^{*R}_{\parallel_0} - A^R_{\parallel_1}A^{*R}_{\perp_0} - \{R \leftrightarrow L\}), \quad (15)$$

$$K_{4sc} = \frac{\alpha_\Lambda}{\sqrt{2}}\mathrm{Re}(A^R_{\perp_1}A^{*R}_{\parallel_0} - A^R_{\parallel_1}A^{*R}_{\perp_0} + \{R \leftrightarrow L\}), \quad (16)$$

$$K_{4s} = \frac{\alpha_\Lambda}{\sqrt{2}}\mathrm{Re}(A^R_{\perp_1}A^{*R}_{\perp_0} - A^R_{\parallel_1}A^{*R}_{\parallel_0} - \{R \leftrightarrow L\}), \quad (17)$$

where the q^2 dependence of the transversity amplitudes is implied. Since we will be focusing on the muonic mode only, we have ignored the lepton mass in writing the coefficients K_i above. The expressions for K_i, including lepton mass effects, can be found in Ref. [71]. The transversity amplitudes $A_i^{L,R}(q^2)$ in terms of the $\Lambda_b \to \Lambda$ form factors $f_i(q^2)$ (see Sec. IV) and $b \to s\ell^+\ell^-$ Wilson coefficients are given by [71]

$$A^{L,(R)}_{\perp_1} = -\sqrt{2}N\left(f^V_\perp\sqrt{2s_-}C^{L,(R)}_+ + \frac{2m_b}{q^2}f^T_\perp(m_{\Lambda_b}+m_\Lambda)\sqrt{2s_-}C^{\mathrm{eff}}_7\right), \quad (18)$$

$$A^{L,(R)}_{\parallel_1} = \sqrt{2}N\left(f^A_\perp\sqrt{2s_+}C^{L,(R)}_- + \frac{2m_b}{q^2}f^{T5}_\perp(m_{\Lambda_b}-m_\Lambda)\sqrt{2s_+}C^{\mathrm{eff}}_7\right), \quad (19)$$

$$A^{L,(R)}_{\perp_0} = \sqrt{2}N\left(f^V_0(m_{\Lambda_b}+m_\Lambda)\sqrt{\frac{s_-}{q^2}}C^{L,(R)}_+ + \frac{2m_b}{q^2}f^T_0\sqrt{q^2s_-}C^{\mathrm{eff}}_7\right), \quad (20)$$

$$A^{L,(R)}_{\parallel_0} = -\sqrt{2}N\left(f^A_0(m_{\Lambda_b}-m_\Lambda)\sqrt{\frac{s_+}{q^2}}C^{L,(R)}_- + \frac{2m_b}{q^2}f^{T5}_0\sqrt{q^2s_+}C^{\mathrm{eff}}_7\right), \quad (21)$$

where $s_\pm = (m_{\Lambda_b} \pm m_\Lambda)^2 - q^2$, and $C^{L(R)}_\pm$ are combinations of Wilson coefficients,

$$C^{L(R)}_+ = (C^{\mathrm{eff}}_9 \mp C_{10}) + (C'_9 \mp C'_{10}),$$
$$C^{L(R)}_- = (C^{\mathrm{eff}}_9 \mp C_{10}) - (C'_9 \mp C'_{10}), \quad (22)$$

and the normalization constant N, a function of q^2, is given by

$$N(q^2) = \left[\frac{G_F^2|V_{tb}V^*_{ts}|^2\alpha_e^2}{3.2^{11}m^3_{\Lambda_b}\pi^5}q^2\lambda^{1/2}(m^2_{\Lambda_b},m^2_\Lambda,q^2)\beta_\ell\right]^{1/2},$$
$$\beta_\ell = \sqrt{1-\frac{4m^2_\ell}{q^2}}, \quad (23)$$

with $\lambda(a,b,c) = a^2+b^2+c^2-2(ab+bc+ca)$.

In the expressions of K_i, the parity violating decay parameter α_Λ arises through the secondary decay $\Lambda \to p\pi^-$. The corresponding hadronic matrix element is given by [46],

$$\langle p(k_1,s_p)\pi^-(k_2)|(\bar{d}u)_{V-A}(\bar{u}s)_{V-A}|\Lambda(k,s_\Lambda)\rangle = [\bar{u}(k_1,s_p)(\xi\gamma_5+\omega)u(k,s_\Lambda)], \quad (24)$$

which depends on only two parameters, ξ and ω. These can be determined from experimental data on $\Lambda \to p\pi^-$. The decay parameter α_Λ then is given by [46]

$$\alpha_\Lambda = \frac{-2\mathrm{Re}(\omega\xi)}{\sqrt{r_-/r_+}|\xi|^2+\sqrt{r_+/r_-}|\omega|^2}, \quad (25)$$

where $r_\pm = (m_\Lambda \pm m_p)^2 - m^2_\pi$.

To write down the corresponding distribution for CP-conjugated mode $\bar{\Lambda}_b \to \bar{\Lambda}(\to \bar{p}\pi^+)\ell^+\ell^-$, we take the following definition for Euler angles: In the rest frame of the $\overline{\Lambda_b}$, the $\bar{\Lambda}$ is assumed to travel along the $+z$ axis, and θ_Λ is the angle between $\bar{\Lambda}$ and the antiproton in the $(\bar{p}\pi^+)$ rest frame. The lepton angle θ_ℓ is the angle between $\bar{\Lambda}$ and ℓ^-[3] in the dilepton rest frame, and ϕ is the angle between planes of $(\bar{p}\pi^+)$ and the lepton pair. With the above convention, the decay distribution for $\bar{\Lambda}_b \to \bar{\Lambda}(\to \bar{p}\pi^+)\ell^+\ell^-$ is simply obtained from Eq. (6) after the transformation ($\theta_\Lambda \to \theta_\Lambda$, $\theta_\ell = \theta_\ell - \pi$, and $\phi \to -\phi$). This is equivalent to replacing the functions K_i's in Eq. (6) with $\bar{K}_i$'s in the following way:

$$K_{1cc,1ss,2cc,2ss,4sc,3s} \to +\bar{K}_{1cc,1ss,2cc,2ss,4sc,3s}, \quad (26)$$

$$K_{1c,2c,4s,3sc} \to -\bar{K}_{1c,2c,4s,3sc}, \quad (27)$$

where $\bar{K}_i$ equals K_i except for the weak phases conjugated. Additionally, in all but three coefficients, K_{1ss}, K_{1cc}, and K_{1c}, we replace the $\Lambda \to p\pi^-$ decay parameter α_Λ by $\bar{\alpha}_\Lambda$, which corresponds to the CP-conjugated decay $\bar{\Lambda} \to \bar{p}\pi^+$. This replacement follows from the fact that under a CP transformation the Dirac-field bilinears transform as $\bar{\psi}_1\psi_2 \xrightarrow{CP} \bar{\psi}_2\psi_1$, $\bar{\psi}_1\gamma_5\psi_2 \xrightarrow{CP} -\bar{\psi}_2\gamma_5\psi_1$. Therefore, in the expression of $\bar{\Lambda} \to \bar{p}\pi^+$, the hadronic matrix element

[3]Note that direction of ℓ^- is taken as reference for both the decay and CP-conjugated mode. This convention is similar to the one used for mesonic counterpart decay in Ref. [41].

obtained through a CP transformation of Eq. (24), the ξ term picks up a minus sign but the ω term does not. The definition of $\bar{\alpha}_\Lambda$, defined similarly to Eq. (25), then implies $\bar{\alpha}_\Lambda = -\alpha_\Lambda$ under strict CP symmetry. Experimentally measured values $\alpha_\Lambda = 0.7519 \pm 0.0036 \pm 0.0024$ and $\bar{\alpha}_\Lambda = -0.7559 \pm 0.0036 \pm 0.0030$ by the BESIII Collaboration [84] agree well with theory.

IV. *CP*-VIOLATING ASYMMETRIES AND RESULTS

Let $\Gamma(H \to f)$ be the decay rate of $H \to f$ (where H indicates the initial state Λ_b and f indicates the final state) and $\bar{\Gamma}(\bar{H} \to \bar{f})$ be the decay rate of the CP-conjugate mode $\bar{H} \to \bar{f}$. As one needs two interfering decay amplitudes to observe a direct CPV, we write the amplitudes as

$$A[H \to f] = |A_1| e^{i\phi_1^w} e^{i\phi_1^s} + |A_2| e^{i\phi_2^w} e^{i\phi_2^s}, \tag{28}$$

$$A[\bar{H} \to \bar{f}] = |A_1| e^{-i\phi_1^w} e^{i\phi_1^s} + |A_2| e^{-i\phi_2^w} e^{i\phi_2^s}, \tag{29}$$

where $\phi_{1,2}^w$ are the weak phases, $\phi_{1,2}^s$ are the strong phases (arising due to final state interactions), and $|A_{1,2}|$ are the moduli of the interfering matrix elements. The decay rate asymmetry that signals the presence of CPV is

$$\Gamma(H \to f) - \bar{\Gamma}(\bar{H} \to \bar{f}) \propto |A_1||A_2| \sin(\phi_1^s - \phi_2^s) \sin(\phi_1^w - \phi_2^w). \tag{30}$$

As evident from this expression, a nonvanishing CP asymmetry requires that both the relative strong and weak phases of the amplitudes must be nonvanishing. The SM has a finite strong phase emanating from the imaginary part of $C_9^{\rm eff}$, which is generated by the $\bar{q}q$ loops ($q = c, u$) in the current-current operators. However, the weak phase, coming from the CKM elements in the last term of Eq. (5), is doubly Cabibbo suppressed and small. Therefore, the CPV in $b \to s\ell^+\ell^-$ transitions in the SM is expected to be very small.

As discussed in the Introduction, the measurements of several observables associated with the $b \to s\ell^+\ell^-$ current are in tension with the SM, and the global fits to data show large preference to a NP hypothesis over the SM. Except for the direct CP asymmetry $A_{\rm CP}^{K^{(*)}}$ [85] and a few angular CP-asymmetries in $B \to K^*\mu^+\mu^-$ [5] and $B_s \to \phi\mu^+\mu^-$ [7,8], most of the measured $b \to s\ell^+\ell^-$ observables, including the ones that show the tensions with the SM, are CP averaged and therefore are not sensitive to the complex phases of NP. Therefore whether the NP in question is real or complex is not clear at present. To answer this question, one needs to study CP-violating observable in $b \to s\ell^+\ell^-$ transition. To this purpose, we construct several CP-violating observables in $\Lambda_b \to \Lambda\ell^+\ell^-$ decay and investigate their sensitivity to complex NP Wilson coefficients. We follow the results of Ref. [17] which performed a global fit analysis of the $b \to s\mu^+\mu^-$ data to complex Wilson coefficients assuming lepton flavor universal couplings to electrons and muons. In particular, we consider the following two LFU NP scenarios:[4]

(i) Case I: $C_9^{\rm NP} = -1.07 - 0.86i$ (NP in left-handed vector operator only)
(ii) Case II: $C_9^{\rm NP} = -C_{10}^{\rm NP} = -0.58 - 1.21i$ [$SU(2)_L$ invariant NP]

associated with the left-handed operators only. In addition, we will also present results for a NP scenario involving purely right-handed current

(iii) Case III: $C_9' = -C_{10}' = 0.04 + 0.16i$ (right-handed NP)

Case I and case II can significantly improve the theory description of the data. Case III, although it cannot explain tensions in $b \to s$ data (see Ref. [86]), we include it in our analysis to assess the sensitivity of CP asymmetries to right-handed NP.[5]

In order to make numerical predictions of observables, one also needs $\Lambda_b \to \Lambda$ form factors for which we use the lattice QCD results of Ref. [47]. The $\Lambda_b \to \Lambda$ hadronic matrix elements are parametrized in terms of ten form factors[6] $f_{t,0,\perp}^V$, $f_{t,0,\perp}^A$, $f_{0,\perp}^T$, $f_{0,\perp}^{T5}$, which are function of q^2. The lattice calculations are fitted to two z parametrizations: the "nominal" fit and "higher-order" fit. Defining the parameter $z(q^2, t_+)$ as

$$z(q^2, t_+) = \frac{\sqrt{t_+ - q^2} - \sqrt{t_+ - t_0}}{\sqrt{t_+ - q^2} + \sqrt{t_+ - t_0}}, \tag{31}$$

where $t_0 = (m_{\Lambda_b} - m_\Lambda)^2$ and $t_+ = (m_B + m_K)^2$, in the so-called nominal fit the form factor parametrization is given as

$$f(q^2) = \frac{1}{1 - q^2/(m_{\rm pole}^f)^2} \left[a_0^f + a_1^f z(q^2, t_+) \right], \tag{32}$$

while in higher-order fit, the parametrization is given as

$$f(q^2) = \frac{1}{1 - q^2/(m_{\rm pole}^f)^2} \left[a_0^f + a_1^f z(q^2, t_+) + a_2^f (z(q^2, t_+))^2 \right], \tag{33}$$

where values of the coefficients a_i^f and the correlations among them are taken from Ref. [47].

[4]Since Ref. [17] provided only a 1σ range of WC values, in choosing the NP benchmark for our analysis, we take median for the real part but the maximum of the 1σ range for the imaginary part to have maximum CP violation effects.

[5]Combination $C_9 = -C_9'$ involving both left- and right-current NP is also favored [17] by the current data.

[6]Note that the form factor labels used in Ref. [47] are different from labels we use in this paper. These are related as $f_{t,0,\perp}^V = f_{0,+,\perp}$, $f_{t,0,\perp}^A = g_{0,+,\perp}$, $f_{0,\perp}^T = h_{+,\perp}$, and $f_{0,\perp}^{T5} = \tilde{h}_{+,\perp}$.

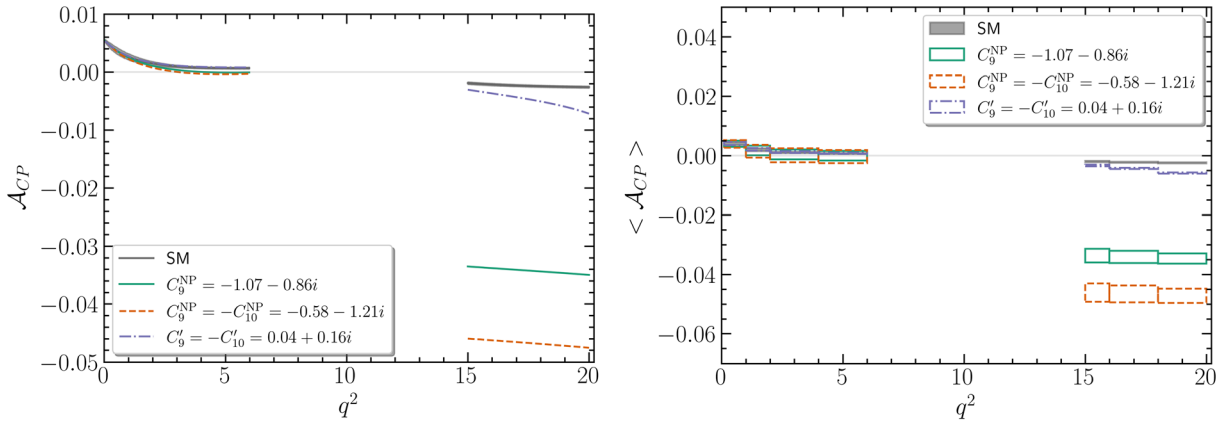

FIG. 1. Predictions for direct CP asymmetry in decay rate ($\mathcal{A}_{CP}$) of $\Lambda_b \to \Lambda\mu^+\mu^-$. In the left plot, the theoretical uncertainties are shown only for the SM case as a dark grey band. In the right plot, the width of rectangle boxes denotes q^2-bin size, and the height of the boxes shows the prediction of the observable together with corresponding (1σ) uncertainties. The same style is used in the rest of figures of this paper.

In our numerical analysis, apart from the already discussed form factors and the Wilson coefficients, we use the results of the CKMfitter Group [87] for values of CKM elements, while particle masses and their lifetime values are taken from the Particle Data Group [88].

With the numerical inputs at our disposal, we make bin-wise predictions of different observables that we describe in the next section. To be precise, the prediction of an observable $\mathcal{O}(q^2)$ in a given bin $q^2 \in [a, b]$ is

$$\langle \mathcal{O} \rangle = \frac{1}{|b-a|} \int_a^b dq^2 \mathcal{O}(q^2). \tag{34}$$

For an observable involving a ratio of two quantities, the binned prediction is obtained after integrating the numerator and denominator separately and then taking their ratio. The two regions of q^2 where we make the predictions are $q^2 \in [0.1, 6]$ and $q^2 \in [15, 20]$. To avoid the charmonium resonances, we refrain from making any prediction in the 6–15 GeV^2 range.

Our numerical determinations are subject to uncertainties coming from different inputs including the form factors. Regarding form factor uncertainties, as described in Ref. [47], we use the nominal fit of Eq. (32) and for an estimation of systematic uncertainties the higher-order fit of Eq. (33) is used. The total uncertainty is obtained after adding statistical and systematic uncertainties in quadrature. In the Appendix we have collected bin-wise predictions of all observables that we describe next.

A. *CP* asymmetry in decay rate

The CP asymmetry in decay rate is defined as

$$\mathcal{A}_{CP} = \frac{d\Gamma/dq^2 - d\bar{\Gamma}/dq^2}{d\Gamma/dq^2 + d\bar{\Gamma}/dq^2}, \tag{35}$$

where $d\Gamma/dq^2$ and $d\bar{\Gamma}/dq^2$ are decay rates of the decay $\Lambda_b \to \Lambda(\to p\pi^-)\mu^+\mu^-$ and its CP-conjugate decay, respectively, which in terms of angular coefficients are defined as

$$\frac{d\Gamma}{dq^2} = 2K_{1ss} + K_{1cc}, \qquad \frac{d\bar{\Gamma}}{dq^2} = 2\bar{K}_{1ss} + \bar{K}_{1cc}. \tag{36}$$

In Fig. 1, we show the $\mathcal{A}_{CP}$ as a function of q^2 (left plot) in the SM and NP scenarios. The corresponding binned predictions are shown in the plot to the right. We find that in the SM the $\mathcal{A}_{CP}$ is, as expected, very small and is $\sim\mathcal{O}(10^{-3})$. In the NP case, we note the following:

(i) $\mathcal{A}_{CP}$ is sensitive to left-handed NP at large q^2 as seen from Fig. 1 where NP cases I and II show a large deviation from the SM. We find that in case II, which has WCs with larger imaginary part, $\mathcal{A}_{CP}$ can be up to 5%.

(ii) We find that $\mathcal{A}_{CP}$ is not sensitive to right-handed currents (NP case III).

(iii) At low q^2, we find $\mathcal{A}_{CP}$ is not sensitive to any of NP scenarios.

B. *CP* asymmetry in longitudinal polarization

We define the CP asymmetry in the longitudinal polarization fraction as the difference between the longitudinal polarization of $\Lambda_b \to \Lambda(\to p\pi^-)\mu^+\mu^-$ [denoted as $F_L(q^2)$] and its CP-conjugate decay [denoted as $\bar{F}_L(q^2)$], normalized by the sum of corresponding decay rates,

$$\mathcal{A}_{F_L} = \frac{F_L(q^2) - \bar{F}_L(q^2)}{d\Gamma/dq^2 + d\bar{\Gamma}/dq^2}, \tag{37}$$

where $F_L(q^2)$ and $\bar{F}_L(q^2)$, in terms of angular coefficients, are given as

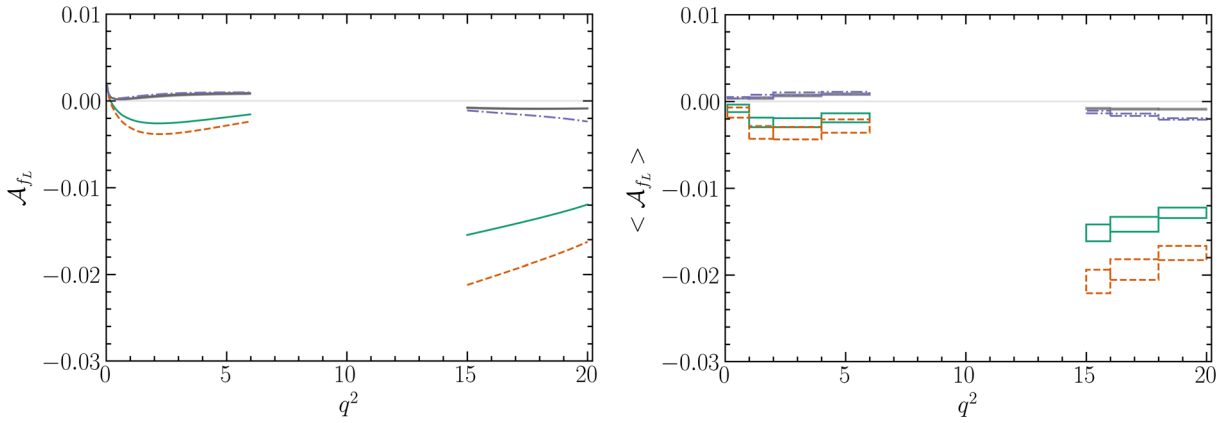

FIG. 2. Predictions for *CP* asymmetry in longitudinal polarization of $\Lambda_b \to \Lambda\mu^+\mu^-$.

$$F_L(q^2) = 2K_{1ss} - K_{1cc},$$
$$\bar{F}_L(q^2) = 2\bar{K}_{1ss} - \bar{K}_{1cc}. \tag{38}$$

Since angular coefficients appearing in $\mathcal{A}_{f_L}$ are the same as in $\mathcal{A}_{CP}$, one expects $\mathcal{A}_{f_L}$ to be sensitive to NP. In Fig. 2, we show results for asymmetry $\mathcal{A}_{f_L}$, and indeed we find that observable is sensitive to left-handed NP (NP cases I and II) while very weakly sensitive to right-handed NP (NP case III). The NP effects are higher in the large q^2 region and $\mathcal{A}_{f_L}$ can be ∼2%. In the low q^2 region, $\mathcal{A}_{f_L}$ remains well below 1%.

C. *CP* asymmetry in forward-backward asymmetries

The decay $\Lambda_b \to \Lambda(\to p\pi^-)\mu^+\mu^-$ offers three types of forward-backward (FB) asymmetries [46]: FB asymmetry ($a_{\rm FB}^{\ell}$) with respect to leptonic angle θ_ℓ, FB asymmetry ($a_{\rm FB}^{\Lambda}$) with respect to hadronic angle θ_Λ, and FB asymmetry ($a_{\rm FB}^{\ell\Lambda}$) with respect to the combination of θ_ℓ and θ_Λ, respectively. In terms of angular coefficients, these are given as

$$a_{\rm FB}^{\ell} = \frac{3}{2}K_{1c}, \qquad a_{\rm FB}^{\Lambda} = \frac{1}{2}(2K_{2ss} + K_{2cc}), \qquad a_{\rm FB}^{\ell\Lambda} = \frac{3}{4}K_{2c}. \tag{39}$$

One can then take the difference between the measurement of the FB asymmetry in the decay $\Lambda_b \to \Lambda(\to p\pi^-)\mu^+\mu^-$ and its *CP* conjugate to define new *CP* asymmetries. These *CP* asymmetries can be accessed by measuring the *CP* asymmetries associated with angular coefficients K_{1c}, K_{2c}, K_{2ss}, and K_{2cc}. To this end, we define the following four *CP* asymmetries:

$$\mathcal{A}_{1c} = \frac{K_{1c}(q^2) - \bar{K}_{1c}(q^2)}{d\Gamma/dq^2 + d\bar{\Gamma}/dq^2}, \tag{40}$$

$$\mathcal{A}_j = \frac{K_j(q^2) + \bar{K}_j(q^2)}{d\Gamma/dq^2 + d\bar{\Gamma}/dq^2}, \quad \text{for } j = 2c, 2ss, 2cc. \tag{41}$$

$\mathcal{A}_{1c}$ and $\mathcal{A}_{2c}$ are equivalent to *CP* asymmetries in $a_{\rm FB}^{\ell}$ and $a_{\rm FB}^{\ell\Lambda}$ up to a normalization constant, while the *CP* asymmetry in $a_{\rm FB}^{\Lambda}$ can be determined from combined measurements of $\mathcal{A}_{2ss}$ and $\mathcal{A}_{2cc}$. Also, note that $\mathcal{A}_{1c}$ involves the difference of K_{1c} and $\bar{K}_{1c}$, while the other *CP* asymmetries involve the sum of corresponding coefficients. This is because the angular coefficients in Eqs. (8)–(17) are proportional to the decay parameter α_Λ (or $\bar{\alpha}_\Lambda$ in the case of the *CP*-conjugate mode). As discussed in the previous section, $\alpha_\Lambda \simeq -\bar{\alpha}_\Lambda$ experimentally, therefore it is the combination $K_j + \bar{K}_j$ ($j = 2c, 2ss, 2cc, 3s, 3sc, 4s, 4sc$) that vanishes in the case of purely real WCs.

In Fig. 3, we show results for $\mathcal{A}_{1c}$, $\mathcal{A}_{2c}$, $\mathcal{A}_{2cc}$, and $\mathcal{A}_{2ss}$. We note the following:

(i) *CP* asymmetry $\mathcal{A}_{1c}$ is sensitive to C_{10}, while no sensitivity to vector and right-handed current is found. We find that in NP case II, which has nonzero $C_{10}^{\rm NP}$, the value of $\mathcal{A}_{1c}$ can be at ∼1.3% level in the large q^2 region. In other NP cases considered, $\mathcal{A}_{1c}$ remain indistinguishable from the SM.

(ii) For the asymmetry $\mathcal{A}_{2c}$, we observe similar NP sensitivity as in $\mathcal{A}_{1c}$ except that the sign of the asymmetry is opposite to that of $\mathcal{A}_{1c}$. We also note that $\mathcal{A}_{2c}$ is largest (∼1.3%) at the kinematic end point $q^2 \sim 20$ GeV^2.

(iii) In contrast, the asymmetries $\mathcal{A}_{2ss}$ and $\mathcal{A}_{2ss}$ are sensitive to C_9, while no sensitivity to axial vector and right-handed currents is found. Both asymmetries are found to be ∼1% in the large q^2 region, with $\mathcal{A}_{2ss}$ being somewhat slightly larger.

D. More *CP* asymmetries

One can define four more *CP* asymmetries associated with angular coefficients K_{3s}, K_{3sc}, K_{4s}, and K_{4sc}, respectively,

$$\mathcal{A}_j = \frac{K_j(q^2) + \bar{K}_j(q^2)}{d\Gamma/dq^2 + d\bar{\Gamma}/dq^2}, \quad \text{for } j = 3s, 3sc, 4s, 4sc. \tag{42}$$

In Fig. 4 we show the results for these *CP* asymmetries and make the following observations:

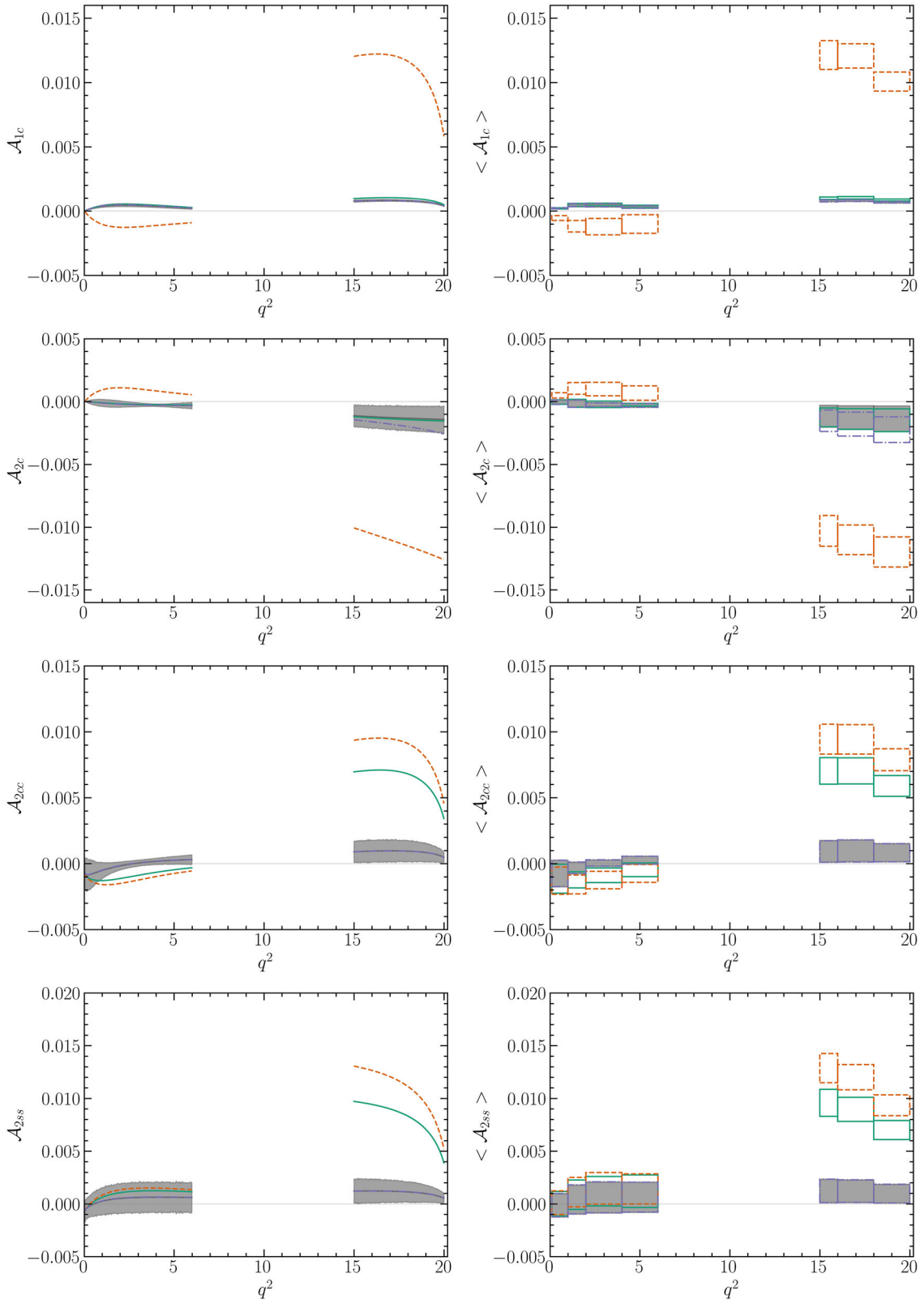

FIG. 3. Predictions for *CP* asymmetries $\mathcal{A}_{1c}$, $\mathcal{A}_{2c}$, $\mathcal{A}_{2cc}$, and $\mathcal{A}_{2ss}$.

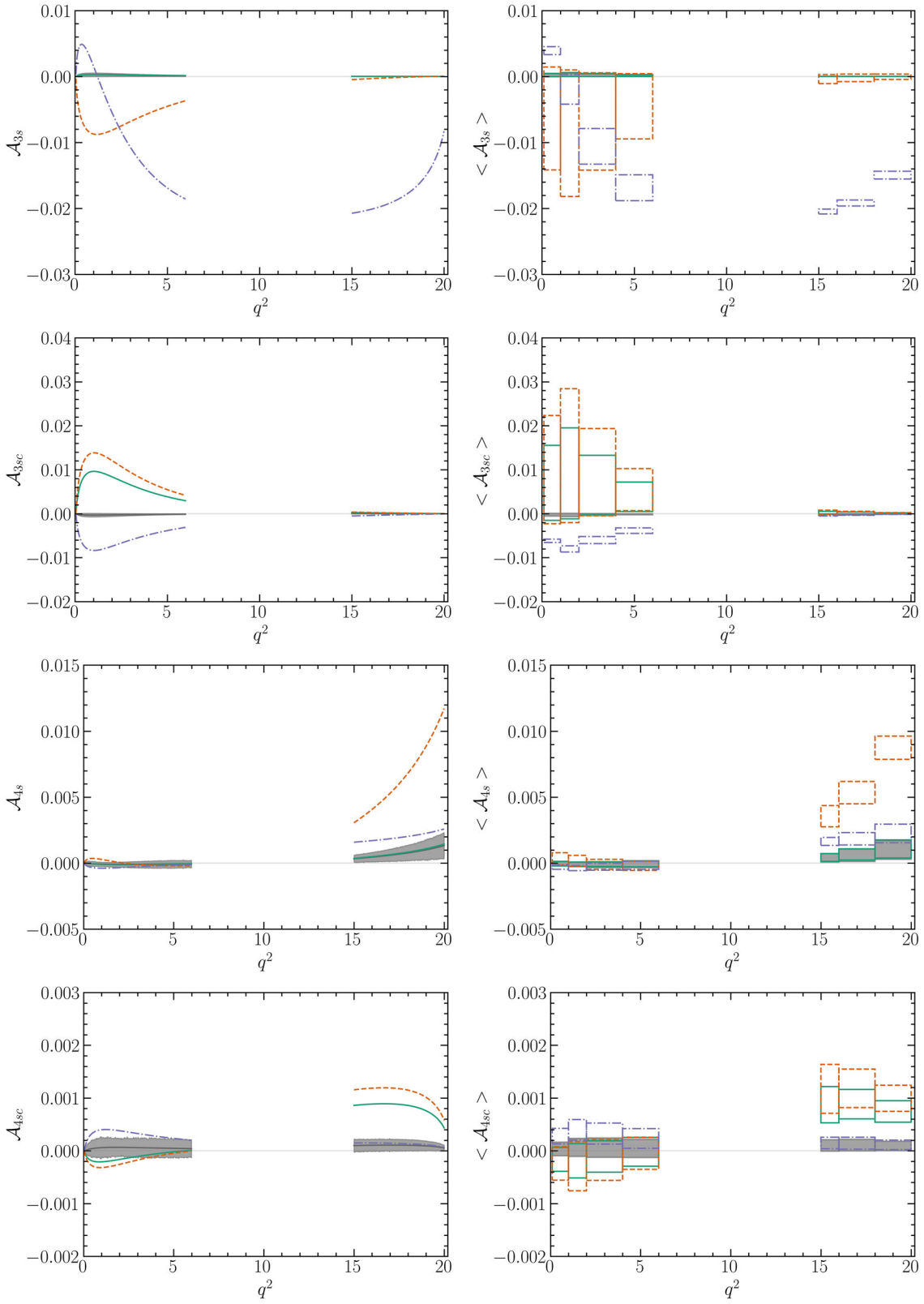

FIG. 4. Predictions for *CP* asymmetries $\mathcal{A}_{3s}$, $\mathcal{A}_{3sc}$, $\mathcal{A}_{4s}$, and $\mathcal{A}_{4sc}$.

(i) We find $\mathcal{A}_{3s}$ to be sensitive to right-handed currents (NP case III) in both low and large q^2 regions, where it can be up to ∼2%. It is also mildly sensitive to C_{10} in the low q^2 region, but has large theoretical uncertainties, as can be seen from low q^2 bins. Another point worth mentioning is that there is zero crossing in the low q^2 region of $\mathcal{A}_{3s}$ for the right-handed NP scenario (case III), while no such behavior is seen in left-handed NP scenarios.

(ii) In case of $\mathcal{A}_{3sc}$, we find the CP asymmetry to be sensitive to C_9 as well as to the right-handed NP case, with its size being ∼1%–3% in the low q^2 region. At large q^2, the CP asymmetry remains negligible.

(iii) For $\mathcal{A}_{4s}$, we find that the asymmetry is sensitive to C_{10} at large q^2. The CP asymmetry remains SM-like in cases with NP in C_9 or right-handed NP. In NP case II (which has nonzero C_{10}), $\mathcal{A}_{4s}$ can be ∼1%.

(iv) On the other hand, for $\mathcal{A}_{4sc}$ we find that the observable is most sensitive to C_9 (NP cases I and II), but the asymmetry remains very small, at $\mathcal{O}(10^{-3})$.

V. CONCLUSION

The experimental data on the $b \to s\ell^+\ell^-$ transitions hints towards the presence of NP that is lepton flavor universal in nature. However, the CP properties of the possible underlying NP is unknown. One concrete way to answer this question is provided by the measurements of CP-violating asymmetries associated with the $b \to s\ell^+\ell^-$ transitions. In the SM, the CPV in the $b \to s\ell^+\ell^-$ transition is very small, but can be enhanced in many NP models. Thus, measurements of sizable $b \to s\ell^+\ell^-$ CP asymmetries are highly motivated. With this in mind, in this paper, we have investigated in a model-independent fashion the prospects of probing CP-violating NP in $\Lambda_b \to \Lambda(\to p\pi^-)\mu^+\mu^-$ decay. To this end, we list all the CP asymmetries offered by the angular distribution of an unpolarized Λ_b decay $\Lambda_b \to \Lambda(\to p\pi^-)\mu^+\mu^-$. We then present their determinations in the SM and several NP scenarios motivated by the present global fits to $b \to s\ell^+\ell^-$ data. We find that several of the CP asymmetries, depending on their NP sensitivity and q^2 region, can be enhanced to a few percent level. More importantly, we find that the measurements of these CP asymmetries can provide new methods to not only probe but also potentially distinguish NP cases discussed in the paper. Therefore, the CP asymmetries in $\Lambda_b \to \Lambda(\to p\pi^-)\mu^+\mu^-$ provide new avenues to cross-check the SM and, in conjunction with CP asymmetries of $B \to K^*\ell^+\ell^-$, can play a useful role in searching NP in $b \to s\ell^+\ell^-$ transitions.

ACKNOWLEDGMENTS

D. D. would like to thank the Department of Science and Technology (DST), Government of India for the INSPIRE Faculty Award (Grant No. IFA16-PH170). D. D. also thanks the Institute for Theoretical Physics III, University of Stuttgart for kind hospitality during various stages of the work. J. D. acknowledges the Council of Scientific and Industrial Research (CSIR), Government of India, for the SRF fellowship grant with File No. 09/045 (1511)/ 2017-EMR-I. J. D. also would like to acknowledge Research Grant No. SERB/CRG/004889/SGBKC/2022/04 of the Science and Engineering Research Board (SERB), India, for partial financial support. The work of G. K. is supported by National Science and Technology Council (NSTC) 111-2639-M-002-002-ASP of Taiwan. N. S. would like to acknowledge support from the UK Science and Technology Facilities Council (STFC).

APPENDIX: PREDICTION OF CP ASYMMETRIES

1. $\mathcal{A}_{CP}$ (in units of 10^{-2})

Bin	SM	Case I	Case II	Case III
[0.1, 1]	0.399 ± 0.052	0.401 ± 0.104	0.389 ± 0.129	0.405 ± 0.052
[1, 2]	0.197 ± 0.046	0.170 ± 0.165	0.141 ± 0.216	0.209 ± 0.047
[2, 4]	0.098 ± 0.024	0.038 ± 0.168	0.005 ± 0.237	0.112 ± 0.030
[4, 6]	0.066 ± 0.017	-0.010 ± 0.162	-0.038 ± 0.224	0.079 ± 0.020
[1.1, 6]	0.098 ± 0.021	0.037 ± 0.165	0.006 ± 0.223	0.111 ± 0.025
[15, 16]	-0.201 ± 0.021	-3.367 ± 0.227	-4.614 ± 0.311	-0.335 ± 0.029
[16, 18]	-0.229 ± 0.021	-3.409 ± 0.207	-4.659 ± 0.283	-0.433 ± 0.024
[18, 20]	-0.250 ± 0.018	-3.464 ± 0.173	-4.720 ± 0.240	-0.590 ± 0.019
[15, 20]	-0.231 ± 0.019	-3.420 ± 0.197	-4.671 ± 0.283	-0.467 ± 0.024

2. $\mathcal{A}_{f_L}$ (in units of 10^{-2})

Bin	SM	Case I	Case II	Case III
[0.1, 1]	0.033 ± 0.003	-0.081 ± 0.043	-0.130 ± 0.059	0.042 ± 0.007
[1, 2]	0.039 ± 0.011	-0.244 ± 0.055	-0.358 ± 0.074	0.058 ± 0.018
[2, 4]	0.068 ± 0.012	-0.247 ± 0.052	-0.367 ± 0.073	0.087 ± 0.018
[4, 6]	0.084 ± 0.011	-0.189 ± 0.053	-0.284 ± 0.078	0.097 ± 0.014
[1.1, 6]	0.071 ± 0.011	-0.220 ± 0.052	-0.328 ± 0.075	0.087 ± 0.016
[15, 16]	-0.084 ± 0.009	-1.516 ± 0.098	-2.076 ± 0.136	-0.123 ± 0.015
[16, 18]	-0.090 ± 0.008	-1.419 ± 0.085	-1.938 ± 0.118	-0.155 ± 0.013
[18, 20]	-0.090 ± 0.007	-1.285 ± 0.061	-1.750 ± 0.083	-0.202 ± 0.008
[15, 20]	-0.089 ± 0.008	-1.392 ± 0.079	-1.901 ± 0.105	-0.165 ± 0.012

3. $\mathcal{A}_{1c}$ (in units of 10^{-2})

Bin	SM	Case I	Case II	Case III
[0.1, 1]	0.020 ± 0.004	0.021 ± 0.004	-0.055 ± 0.019	0.022 ± 0.005
[1, 2]	0.044 ± 0.010	0.048 ± 0.011	-0.118 ± 0.045	0.046 ± 0.010
[2, 4]	0.044 ± 0.011	0.051 ± 0.011	-0.122 ± 0.064	0.046 ± 0.013
[4, 6]	0.030 ± 0.009	0.036 ± 0.010	-0.100 ± 0.072	0.032 ± 0.010
[1.1, 6]	0.037 ± 0.009	0.044 ± 0.010	-0.111 ± 0.065	0.040 ± 0.010
[15, 16]	0.080 ± 0.008	0.100 ± 0.010	1.213 ± 0.112	0.080 ± 0.008
[16, 18]	0.083 ± 0.007	0.103 ± 0.009	1.206 ± 0.094	0.082 ± 0.007
[18, 20]	0.069 ± 0.006	0.086 ± 0.007	1.006 ± 0.074	0.069 ± 0.006
[15, 20]	0.078 ± 0.007	0.096 ± 0.008	1.137 ± 0.084	0.077 ± 0.007

4. $\mathcal{A}_{2c}$ (in units of 10^{-2})

Bin	SM	Case I	Case II	Case III
[0.1, 1]	-0.004 ± 0.017	-0.004 ± 0.017	0.048 ± 0.021	-0.006 ± 0.017
[1, 2]	-0.015 ± 0.029	-0.015 ± 0.032	0.104 ± 0.047	-0.018 ± 0.029
[2, 4]	-0.025 ± 0.015	-0.023 ± 0.025	0.099 ± 0.053	-0.026 ± 0.015
[4, 6]	-0.031 ± 0.015	-0.026 ± 0.010	0.068 ± 0.057	-0.031 ± 0.015
[1.1, 6]	-0.026 ± 0.010	-0.023 ± 0.018	0.086 ± 0.052	-0.027 ± 0.010
[15, 16]	-0.118 ± 0.087	-0.126 ± 0.075	-1.03 ± 0.123	-0.153 ± 0.086
[16, 18]	-0.128 ± 0.094	-0.138 ± 0.082	-1.101 ± 0.118	-0.180 ± 0.094
[18, 20]	-0.138 ± 0.102	-0.150 ± 0.091	-1.197 ± 0.120	-0.224 ± 0.102
[15, 20]	-0.129 ± 0.095	-0.140 ± 0.086	-1.12 ± 0.122	-0.190 ± 0.095

5. $\mathcal{A}_{2cc}$ (in units of 10^{-2})

Bin	SM	Case I	Case II	Case III
[0.1, 1]	-0.076 ± 0.101	-0.115 ± 0.110	-0.129 ± 0.103	-0.074 ± 0.100
[1, 2]	-0.034 ± 0.044	-0.123 ± 0.061	-0.158 ± 0.072	-0.031 ± 0.043
[2, 4]	0.003 ± 0.024	-0.089 ± 0.055	-0.124 ± 0.066	0.005 ± 0.024
[4, 6]	0.025 ± 0.030	-0.047 ± 0.051	-0.075 ± 0.067	0.026 ± 0.030
[1.1, 6]	0.008 ± 0.029	-0.075 ± 0.047	-0.107 ± 0.064	0.010 ± 0.029
[15, 16]	0.092 ± 0.082	0.703 ± 0.100	0.944 ± 0.114	0.092 ± 0.082
[16, 18]	0.096 ± 0.083	0.702 ± 0.099	0.941 ± 0.111	0.096 ± 0.083
[18, 20]	0.083 ± 0.069	0.589 ± 0.079	0.788 ± 0.082	0.082 ± 0.069
[15, 20]	0.091 ± 0.078	0.663 ± 0.087	0.888 ± 0.104	0.090 ± 0.078

6. $\mathcal{A}_{2ss}$ (in units of 10^{-2})

Bin	SM	Case I	Case II	Case III
[0.1, 1]	-0.014 ± 0.111	0.001 ± 0.116	0.011 ± 0.112	-0.013 ± 0.110
[1, 2]	0.040 ± 0.137	0.087 ± 0.140	0.111 ± 0.139	0.043 ± 0.137
[2, 4]	0.060 ± 0.147	0.120 ± 0.140	0.147 ± 0.150	0.062 ± 0.146
[4, 6]	0.062 ± 0.142	0.120 ± 0.154	0.143 ± 0.143	0.064 ± 0.142
[1.1, 6]	0.058 ± 0.149	0.115 ± 0.148	0.139 ± 0.152	0.060 ± 0.149
[15, 16]	0.122 ± 0.111	0.958 ± 0.128	1.286 ± 0.139	0.123 ± 0.112
[16, 18]	0.119 ± 0.106	0.896 ± 0.114	1.201 ± 0.120	0.121 ± 0.107
[18, 20]	0.096 ± 0.088	0.699 ± 0.090	0.934 ± 0.098	0.097 ± 0.089
[15, 20]	0.112 ± 0.097	0.840 ± 0.108	1.125 ± 0.123	0.113 ± 0.097

7. $\mathcal{A}_{3s}$ (in units of 10^{-2})

Bin	SM	Case I	Case II	Case III
[0.1, 1]	0.021 ± 0.023	0.022 ± 0.024	-0.636 ± 0.780	0.392 ± 0.061
[1, 2]	0.026 ± 0.026	0.029 ± 0.030	-0.859 ± 0.959	-0.194 ± 0.226
[2, 4]	0.020 ± 0.020	0.023 ± 0.023	-0.680 ± 0.738	-1.059 ± 0.270
[4, 6]	0.013 ± 0.012	0.015 ± 0.015	-0.451 ± 0.494	-1.686 ± 0.196
[1.1, 6]	0.017 ± 0.018	0.020 ± 0.021	-0.604 ± 0.683	-1.223 ± 0.244
[15, 16]	0.002 ± 0.002	0.002 ± 0.002	-0.039 ± 0.068	-2.047 ± 0.038
[16, 18]	0.001 ± 0.001	0.001 ± 0.002	-0.020 ± 0.056	-1.917 ± 0.045
[18, 20]	0.000 ± 0.001	0.001 ± 0.001	-0.002 ± 0.040	-1.494 ± 0.058
[15, 20]	0.001 ± 0.001	0.001 ± 0.001	-0.018 ± 0.051	-1.796 ± 0.046

8. $\mathcal{A}_{3sc}$ (in units of 10^{-2})

Bin	SM	Case I	Case II	Case III
[0.1, 1]	-0.023 ± 0.032	0.702 ± 0.853	1.003 ± 1.232	-0.618 ± 0.038
[1, 2]	-0.030 ± 0.038	0.918 ± 1.034	1.321 ± 1.522	-0.802 ± 0.069
[2, 4]	-0.022 ± 0.025	0.658 ± 0.667	0.945 ± 0.992	-0.600 ± 0.081
[4, 6]	-0.013 ± 0.013	0.384 ± 0.333	0.547 ± 0.479	-0.384 ± 0.063
[1.1, 6]	-0.019 ± 0.022	0.575 ± 0.571	0.822 ± 0.826	-0.530 ± 0.073
[15, 16]	-0.001 ± 0.002	0.023 ± 0.033	0.032 ± 0.047	-0.046 ± 0.006
[16, 18]	-0.001 ± 0.001	0.014 ± 0.023	0.019 ± 0.035	-0.031 ± 0.004
[18, 20]	-0.000 ± 0.001	0.005 ± 0.012	0.007 ± 0.017	-0.013 ± 0.002
[15, 20]	-0.000 ± 0.001	0.013 ± 0.021	0.017 ± 0.029	-0.028 ± 0.004

9. $\mathcal{A}_{4s}$ (in units of 10^{-2})

Bin	SM	Case I	Case II	Case III
[0.1, 1]	-0.004 ± 0.016	-0.004 ± 0.017	0.031 ± 0.048	-0.029 ± 0.017
[1, 2]	-0.010 ± 0.016	-0.008 ± 0.016	0.017 ± 0.042	-0.037 ± 0.019
[2, 4]	-0.011 ± 0.024	-0.008 ± 0.017	-0.009 ± 0.038	-0.027 ± 0.026
[4, 6]	-0.008 ± 0.027	-0.005 ± 0.022	-0.020 ± 0.035	-0.015 ± 0.031
[1.1, 6]	-0.010 ± 0.023	-0.007 ± 0.017	-0.010 ± 0.040	-0.023 ± 0.025
[15, 16]	0.039 ± 0.032	0.042 ± 0.029	0.356 ± 0.081	0.165 ± 0.031
[16, 18]	0.060 ± 0.049	0.065 ± 0.042	0.534 ± 0.084	0.185 ± 0.047
[18, 20]	0.100 ± 0.071	0.108 ± 0.069	0.875 ± 0.088	0.225 ± 0.070
[15, 20]	0.070 ± 0.055	0.076 ± 0.044	0.617 ± 0.082	0.195 ± 0.054

10. $\mathcal{A}_{4sc}$ (in units of 10^{-2})

Bin	SM	Case I	Case II	Case III
[0.1, 1]	0.003 ± 0.013	-0.016 ± 0.023	-0.024 ± 0.032	0.028 ± 0.015
[1, 2]	0.006 ± 0.017	-0.019 ± 0.033	-0.029 ± 0.047	0.040 ± 0.020
[2, 4]	0.006 ± 0.019	-0.011 ± 0.030	-0.017 ± 0.038	0.033 ± 0.020
[4, 6]	0.005 ± 0.017	-0.002 ± 0.027	-0.005 ± 0.030	0.023 ± 0.019
[1.1, 6]	0.005 ± 0.017	-0.008 ± 0.027	-0.013 ± 0.033	0.029 ± 0.018
[15, 16]	0.010 ± 0.011	0.087 ± 0.034	0.117 ± 0.046	0.015 ± 0.011
[16, 18]	0.011 ± 0.011	0.088 ± 0.028	0.118 ± 0.037	0.014 ± 0.011
[18, 20]	0.009 ± 0.009	0.075 ± 0.020	0.100 ± 0.025	0.011 ± 0.009
[15, 20]	0.010 ± 0.011	0.083 ± 0.026	0.112 ± 0.034	0.013 ± 0.011

[1] C. Abel *et al.*, Measurement of the Permanent Electric Dipole Moment of the Neutron, Phys. Rev. Lett. **124**, 081803 (2020).

[2] A. D. Sakharov, Violation of CP invariance, C asymmetry, and baryon asymmetry of the universe, Pis'ma Zh. Eksp. Teor. Fiz. **5**, 32 (1967).

[3] R. Aaij *et al.* (LHCb Collaboration), Measurement of Form-Factor-Independent Observables in the Decay $B^0 \to K^{*0}\mu^+\mu^-$, Phys. Rev. Lett. **111**, 191801 (2013).

[4] R. Aaij *et al.* (LHCb Collaboration), Differential branching fractions and isospin asymmetries of $B \to K^{(*)}\mu^+\mu^-$ decays, J. High Energy Phys. 06 (2014) 133.

[5] R. Aaij *et al.* (LHCb Collaboration), Angular analysis of the $B^0 \to K^{*0}\mu^+\mu^-$ decay using 3 fb^{-1} of integrated luminosity, J. High Energy Phys. 02 (2016) 104.

[6] R. Aaij *et al.* (LHCb Collaboration), Measurement of CP-Averaged Observables in the $B^0 \to K^{*0}\mu^+\mu^-$ Decay, Phys. Rev. Lett. **125**, 011802 (2020).

[7] R. Aaij *et al.* (LHCb Collaboration), Angular analysis and differential branching fraction of the decay $B_s^0 \to \phi\mu^+\mu^-$, J. High Energy Phys. 09 (2015) 179.

[8] R. Aaij *et al.* (LHCb Collaboration), Angular analysis of the rare decay $B_s^0 \to \phi\mu^+\mu^-$, J. High Energy Phys. 11 (2021) 043.

[9] G. Hiller and F. Kruger, More model-independent analysis of $b \to s$ processes, Phys. Rev. D **69**, 074020 (2004).

[10] C. Bobeth, G. Hiller, and G. Piranishvili, Angular distributions of $\bar{B} \to \bar{K}\ell^+\ell^-$ decays, J. High Energy Phys. 12 (2007) 040.

[11] LHCb Collaboration, Test of lepton universality in $b \to s\ell^+\ell^-$ decays, arXiv:2212.09152.

[12] LHCb Collaboration, Measurement of lepton universality parameters in $B^+ \to K^+\ell^+\ell^-$ and $B^0 \to K^{*0}\ell^+\ell^-$ decays, arXiv:2212.09153.

[13] R. Aaij *et al.* (LHCb Collaboration), Test of Lepton Universality Using $B^+ \to K^+\ell^+\ell^-$ Decays, Phys. Rev. Lett. **113**, 151601 (2014).

[14] R. Aaij *et al.* (LHCb Collaboration), Test of lepton universality with $B^0 \to K^{*0}\ell^+\ell^-$ decays, J. High Energy Phys. 08 (2017) 055.

[15] R. Aaij *et al.* (LHCb Collaboration), Search for Lepton-Universality Violation in $B^+ \to K^+\ell^+\ell^-$ Decays, Phys. Rev. Lett. **122**, 191801 (2019).

[16] R. Aaij *et al.* (LHCb Collaboration), Test of lepton universality in beauty-quark decays, Nat. Phys. **18**, 277 (2022).

[17] N. R. Singh Chundawat, CP violation in $b \to s\ell\ell$: A model independent analysis, Phys. Rev. D **107**, 075014 (2023).

[18] A. Greljo, J. Salko, A. Smolkovič, and P. Stangl, Rare b decays meet high-mass Drell-Yan, J. High Energy Phys. 05 (2023) 087.

[19] M. Algueró, A. Biswas, B. Capdevila, S. Descotes-Genon, J. Matias, and M. Novoa-Brunet, To (b)e or not to (b)e: No electrons at LHCb, arXiv:2304.07330.

[20] S. Descotes-Genon, J. Matias, and J. Virto, Understanding the $B \to K^*\mu^+\mu^-$ anomaly, Phys. Rev. D **88**, 074002 (2013).

[21] W. Altmannshofer and D. M. Straub, New physics in $B \to K^*\mu\mu$?, Eur. Phys. J. C **73**, 2646 (2013).

[22] F. Beaujean, C. Bobeth, and D. van Dyk, Comprehensive Bayesian analysis of rare (semi)leptonic and radiative B decays, Eur. Phys. J. C **74**, 2897 (2014); **74**, 3179(E) (2014).

[23] T. Hurth and F. Mahmoudi, On the LHCb anomaly in $B \to K^*\ell^+\ell^-$, J. High Energy Phys. 04 (2014) 097.

[24] T. Hurth, F. Mahmoudi, and S. Neshatpour, Global fits to $b \to s\ell\ell$ data and signs for lepton non-universality, J. High Energy Phys. 12 (2014) 053.

[25] W. Altmannshofer and D. M. Straub, New physics in $b \to s$ transitions after LHC run 1, Eur. Phys. J. C **75**, 382 (2015).

[26] S. Descotes-Genon, L. Hofer, J. Matias, and J. Virto, Global analysis of $b \to s\ell\ell$ anomalies, J. High Energy Phys. 06 (2016) 092.

[27] B. Capdevila, A. Crivellin, S. Descotes-Genon, J. Matias, and J. Virto, Patterns of new physics in $b \to s\ell^+\ell^-$ transitions in the light of recent data, J. High Energy Phys. 01 (2018) 093.

[28] G. D'Amico, M. Nardecchia, P. Panci, F. Sannino, A. Strumia, R. Torre, and A. Urbano, Flavour anomalies after the R_{K^*} measurement, J. High Energy Phys. 09 (2017) 010.

[29] M. Algueró, B. Capdevila, A. Crivellin, S. Descotes-Genon, P. Masjuan, J. Matias, M. Novoa Brunet, and J. Virto, Emerging patterns of new physics with and without lepton

flavour universal contributions, Eur. Phys. J. C **79**, 714 (2019); **80**, 511(A) (2020).
[30] K. Kowalska, D. Kumar, and E. M. Sessolo, Implications for new physics in $b \to s\mu\mu$ transitions after recent measurements by Belle and LHCb, Eur. Phys. J. C **79**, 840 (2019).
[31] A. K. Alok, A. Dighe, S. Gangal, and D. Kumar, Continuing search for new physics in $b \to s\mu\mu$ decays: Two operators at a time, J. High Energy Phys. 06 (2019) 089.
[32] T. Hurth, F. Mahmoudi, and S. Neshatpour, Model independent analysis of the angular observables in $B^0 \to K^{*0}\mu^+\mu^-$ and $B^+ \to K^{*+}\mu^+\mu^-$, Phys. Rev. D **103**, 095020 (2021).
[33] L.-S. Geng, B. Grinstein, S. Jäger, S.-Y. Li, J. Martin Camalich, and R.-X. Shi, Implications of new evidence for lepton-universality violation in $b \to s\ell^+\ell^-$ decays, Phys. Rev. D **104**, 035029 (2021).
[34] W. Altmannshofer and P. Stangl, New physics in rare B decays after Moriond 2021, Eur. Phys. J. C **81**, 952 (2021).
[35] M. Algueró, B. Capdevila, S. Descotes-Genon, J. Matias, and M. Novoa-Brunet, $b \to s\ell^+\ell^-$ global fits after R_{K_S} and $R_{K^{*+}}$, Eur. Phys. J. C **82**, 326 (2022).
[36] M. Ciuchini, M. Fedele, E. Franco, A. Paul, L. Silvestrini, and M. Valli, Constraints on lepton universality violation from rare B decays, Phys. Rev. D **107**, 055036 (2023).
[37] R. Fleischer, E. Malami, A. Rehult, and K. K. Vos, New perspectives for testing electron-muon universality, arXiv:2303.08764.
[38] C. Bobeth, G. Hiller, and G. Piranishvili, *CP* asymmetries in bar $B \to \bar{K}^*(\to \bar{K}\pi)\overline{\ell}\ell$ and untagged $\bar{B}_s$, $B_s \to \phi(\to K^+K^-)\overline{\ell}\ell$ decays at NLO, J. High Energy Phys. 07 (2008) 106.
[39] F. Kruger, L. M. Sehgal, N. Sinha, and R. Sinha, Angular distribution and *CP* asymmetries in the decays $\bar{B} \to K^-\pi^+e^-e^+$ and $\bar{B} \to \pi^-\pi^+e^-e^+$, Phys. Rev. D **61**, 114028 (2000); **63**, 019901(E) (2001).
[40] C. S. Kim and T. Yoshikawa, Systematic analysis of $B \to K\pi l^+l^-$ decay through angular decomposition, arXiv:0711.3880.
[41] W. Altmannshofer, P. Ball, A. Bharucha, A. J. Buras, D. M. Straub, and M. Wick, Symmetries and asymmetries of $B \to K^*\mu^+\mu^-$ decays in the standard model and beyond, J. High Energy Phys. 01 (2009) 019.
[42] A. K. Alok, A. Datta, A. Dighe, M. Duraisamy, D. Ghosh, and D. London, New physics in $b \to s\mu^+\mu^-$: *CP*-violating observables, J. High Energy Phys. 11 (2011) 122.
[43] A. K. Alok, B. Bhattacharya, D. Kumar, J. Kumar, D. London, and S. U. Sankar, New physics in $b \to s\mu^+\mu^-$: Distinguishing models through *CP*-violating effects, Phys. Rev. D **96**, 015034 (2017).
[44] D. Bečirević, S. Fajfer, N. Košnik, and A. Smolkovič, Enhanced *CP* asymmetries in $B \to K\mu^+\mu^-$, Eur. Phys. J. C **80**, 940 (2020).
[45] S. N. Gangal, Enhancement of direct *CP* asymmetry in Z' models, arXiv:2209.02476.
[46] P. Böer, T. Feldmann, and D. van Dyk, Angular analysis of the decay $\Lambda_b \to \Lambda(\to N\pi)\ell^+\ell^-$, J. High Energy Phys. 01 (2015) 155.
[47] W. Detmold and S. Meinel, $\Lambda_b \to \Lambda\ell^+\ell^-$ form factors, differential branching fraction, and angular observables from lattice QCD with relativistic b quarks, Phys. Rev. D **93**, 074501 (2016).
[48] T. Aaltonen *et al.* (CDF Collaboration), Observation of the Baryonic Flavor-Changing Neutral Current Decay $\Lambda_b \to \Lambda\mu^+\mu^-$, Phys. Rev. Lett. **107**, 201802 (2011).
[49] R. Aaij *et al.* (LHCb Collaboration), Angular moments of the decay $\Lambda_b^0 \to \Lambda\mu^+\mu^-$ at low hadronic recoil, J. High Energy Phys. 09 (2018) 146.
[50] T. Blake and M. Kreps, Angular distribution of polarised Λ_b baryons decaying to $\Lambda\ell^+\ell^-$, J. High Energy Phys. 11 (2017) 138.
[51] D. Das and R. Sain, Polarized Λb baryon decay to $p\pi$ and a dilepton pair, Phys. Rev. D **104**, 013002 (2021).
[52] R. Aaij *et al.* (LHCb Collaboration), Differential branching fraction and angular analysis of $\Lambda_b^0 \to \Lambda\mu^+\mu^-$ decays, J. High Energy Phys. 06 (2015) 115; 09 (2018) 145(E).
[53] C.-S. Huang and H.-G. Yan, Exclusive rare decays of heavy baryons to light baryons: $\Lambda_b \to \Lambda\gamma$ and $\Lambda_b \to \Lambda l^+l^-$, Phys. Rev. D **59**, 114022 (1999); **61**, 039901(E) (2000).
[54] C.-H. Chen and C. Q. Geng, Lepton asymmetries in heavy baryon decays of $\Lambda_b \to \Lambda l^+l^-$, Phys. Lett. B **516**, 327 (2001).
[55] C.-H. Chen and C. Q. Geng, Rare $\Lambda_b \to \Lambda l^+l^-$ decays with polarized Λ, Phys. Rev. D **63**, 114024 (2001).
[56] T. M. Aliev, A. Ozpineci, M. Savci, and C. Yuce, *T* violation in $\Lambda_b \to \Lambda\ell^+\ell^-$ decay beyond standard model, Phys. Lett. B **542**, 229 (2002).
[57] T. M. Aliev, A. Ozpineci, and M. Savci, New physics effects in $\Lambda_b \to \Lambda\ell^+\ell^-$ decay with lepton polarizations, Phys. Rev. D **65**, 115002 (2002).
[58] T. M. Aliev, A. Ozpineci, and M. Savci, Model independent analysis of Λ baryon polarizations in $\Lambda_b \to \Lambda l^+l^-$ decay, Phys. Rev. D **67**, 035007 (2003).
[59] T. M. Aliev, V. Bashiry, and M. Savci, Forward-backward asymmetries in $\Lambda_b \to \Lambda l^+l^-$ decay beyond the standard model, Nucl. Phys. **B709**, 115 (2005).
[60] T. M. Aliev, V. Bashiry, and M. Savci, Double-lepton polarization asymmetries in $\Lambda_b \to \Lambda l^+l^-$ decay, Eur. Phys. J. C **38**, 283 (2004).
[61] T. M. Aliev and M. Savci, Polarization effects in exclusive semileptonic $\Lambda_b \to \Lambda l^+l^-$ decay, J. High Energy Phys. 05 (2006) 001.
[62] Y.-m. Wang, Y. Li, and C.-D. Lu, Rare decays of $\Lambda_b \to \Lambda + \gamma$ and $\Lambda_b \to \Lambda + l^+l^-$ in the light-cone sum rules, Eur. Phys. J. C **59**, 861 (2009).
[63] T. M. Aliev, K. Azizi, and M. Savci, Analysis of the $\Lambda_b \to \Lambda\ell^+\ell^-$ decay in QCD, Phys. Rev. D **81**, 056006 (2010).
[64] L. Mott and W. Roberts, Rare dileptonic decays of Λ_b in a quark model, Int. J. Mod. Phys. A **27**, 1250016 (2012).
[65] T. Gutsche, M. A. Ivanov, J. G. Korner, V. E. Lyubovitskij, and P. Santorelli, Rare baryon decays $\Lambda_b \to \Lambda l^+l^-(l = e, \mu, \tau)$ and $\Lambda_b \to \Lambda\gamma$: Differential and total rates, lepton- and hadron-side forward-backward asymmetries, Phys. Rev. D **87**, 074031 (2013).
[66] G. Kumar and N. Mahajan, Asymmetries and observables for $\Lambda_b \to \Lambda\ell^+\ell^-$, arXiv:1511.00935.
[67] S. Meinel and D. van Dyk, Using $\Lambda_b \to \Lambda\mu^+\mu^-$ data within a Bayesian analysis of $|\Delta B| = |\Delta S| = 1$ decays, Phys. Rev. D **94**, 013007 (2016).

[68] R. N. Faustov and V. O. Galkin, Rare $\Lambda_b \to \Lambda l^+ l^-$ and $\Lambda_b \to \Lambda\gamma$ decays in the relativistic quark model, Phys. Rev. D **96**, 053006 (2017).

[69] S. Roy, R. Sain, and R. Sinha, Lepton mass effects and angular observables in $\Lambda_b \to \Lambda(\to p\pi)\ell^+\ell^-$, Phys. Rev. D **96**, 116005 (2017).

[70] D. Das, Model independent new physics analysis in $\Lambda_b \to \Lambda\mu^+\mu^-$ decay, Eur. Phys. J. C **78**, 230 (2018).

[71] D. Das, On the angular distribution of $\Lambda_b \to \Lambda(\to N\pi)\tau^+\tau^-$ decay, J. High Energy Phys. 07 (2018) 063.

[72] D. Das, Lepton flavor violating $\Lambda_b \to \Lambda\ell_1\ell_2$ decay, Eur. Phys. J. C **79**, 1005 (2019).

[73] S. Bhattacharya, S. Nandi, S. K. Patra, and R. Sain, Detailed study of the $\Lambda_b \to \Lambda\ell^+\ell^-$ decays in the standard model, Phys. Rev. D **101**, 073006 (2020).

[74] T. Blake, S. Meinel, and D. van Dyk, Bayesian analysis of $b \to s\mu^+\mu^-$ Wilson coefficients using the full angular distribution of $\Lambda_b \to \Lambda(\to p\pi^-)\mu^+\mu^-$ decays, Phys. Rev. D **101**, 035023 (2020).

[75] M. Bordone, M. Rahimi, and K. K. Vos, Lepton flavour violation in rare Λ_b decays, Eur. Phys. J. C **81**, 756 (2021).

[76] B. Grinstein, M. J. Savage, and M. B. Wise, $B \to X_s e^+ e^-$ in the six quark model, Nucl. Phys. **B319**, 271 (1989).

[77] G. Buchalla, A. J. Buras, and M. E. Lautenbacher, Weak decays beyond leading logarithms, Rev. Mod. Phys. **68**, 1125 (1996).

[78] K. G. Chetyrkin, M. Misiak, and M. Munz, Weak radiative B meson decay beyond leading logarithms, Phys. Lett. B **400**, 206 (1997); **425**, 414(E) (1998).

[79] M. Beneke, T. Feldmann, and D. Seidel, Systematic approach to exclusive $B \to Vl^+l^-$, $V\gamma$ decays, Nucl. Phys. **B612**, 25 (2001).

[80] H. H. Asatryan, H. M. Asatrian, C. Greub, and M. Walker, Calculation of two loop virtual corrections to $b \to sl^+l^-$ in the standard model, Phys. Rev. D **65**, 074004 (2002).

[81] C. Greub, V. Pilipp, and C. Schupbach, Analytic calculation of two-loop QCD corrections to $b \to sl^+l^-$ in the high q^2 region, J. High Energy Phys. 12 (2008) 040.

[82] R. Alonso, B. Grinstein, and J. Martin Camalich, $SU(2) \times U(1)$ Gauge Invariance and the Shape of New Physics in Rare B Decays, Phys. Rev. Lett. **113**, 241802 (2014).

[83] F. Beaujean, C. Bobeth, and S. Jahn, Constraints on tensor and scalar couplings from $B \to K\bar{\mu}\mu$ and $B_s \to \bar{\mu}\mu$, Eur. Phys. J. C **75**, 456 (2015).

[84] M. Ablikim *et al.* (BESIII Collaboration), Precise Measurements of Decay Parameters and CP Asymmetry with Entangled $\Lambda - \bar{\Lambda}$ Pairs, Phys. Rev. Lett. **129**, 131801 (2022).

[85] R. Aaij *et al.* (LHCb Collaboration), Measurement of CP asymmetries in the decays $B^0 \to K^{*0}\mu^+\mu^-$ and $B^+ \to K^+\mu^+\mu^-$, J. High Energy Phys. 09 (2014) 177.

[86] A. Carvunis, F. Dettori, S. Gangal, D. Guadagnoli, and C. Normand, On the effective lifetime of $B_s \to \mu\mu\gamma$, J. High Energy Phys. 12 (2021) 078.

[87] J. Charles, A. Hocker, H. Lacker, S. Laplace, F. R. Le Diberder, J. Malcles, J. Ocariz, M. Pivk, and L. Roos (CKMfitter Group), CP violation and the CKM matrix: Assessing the impact of the asymmetric B factories, Eur. Phys. J. C **41**, 1 (2005).

[88] R. L. Workman *et al.* (Particle Data Group), Review of particle physics, Prog. Theor. Exp. Phys. **2022**, 083C01 (2022).